



Научная статья

DOI: 10.15593/perm.mech/2023.3.10

УДК 620.1/.2

ЧИСЛЕННОЕ И ЭКСПЕРИМЕНТАЛЬНОЕ ИССЛЕДОВАНИЕ ОПТИМИЗАЦИИ СТРУКТУРЫ УГЛЕПЛАСТИКА ПО КОЭФФИЦИЕНТУ ТЕПЛООВОГО РАСШИРЕНИЯ

К.А. Пасечник, И.В. Обверткин, А.Ю. Власов

Сибирский университет науки и технологий, Красноярск, Российская Федерация

О СТАТЬЕ

Получена: 13 января 2023 г.

Одобрена: 25 мая 2023 г.

Принята к публикации:

15 июня 2023 г.

Ключевые слова:

оптимизация макроструктуры гибридного композита, стабильно низкий коэффициент теплового расширения композита, МУНТ, PCA, NSGA-II, модель Мори – Танаки.

АННОТАЦИЯ

Исследуется оптимизация макроструктуры для достижения стабильно низкого коэффициента теплового расширения α_x композита с углеродными волокнами. Для ограничения области поиска предложено необходимое условие существования локальных минимумов α_x , выраженное через радиусы гипербол в проектном пространстве угловой ориентации слоев, преобразованном алгоритмом PCA. Анализ вариантов структуры, характеризующихся низким α_x , показывает различную устойчивость к вариативности свойств единичного слоя композита. Выполнена многокритериальная оптимизация. Целевыми функциями являются математическое ожидание $E(\alpha_x)$ и дисперсия $Var(\alpha_x)$. Анализ Парето-фронта и функций плотности распределения вероятности позволяет оценить достижимость расчетного α_x при заданных условиях вариативности свойств единичного слоя композита.

Исследована возможность уменьшения дисперсии распределения α_x путем модификации полимерной матрицы многостенными углеродными нанотрубками (МУНТ) в условиях дезориентации армирующих волокон и вариативности свойств единичного слоя. Модификация микроструктуры полимерного композиционного материала позволяет снизить $Var(\alpha_x)$ на 91,61 % при объемном соотношении МУНТ до 1 %. Требуемые термомеханические свойства достигаются путем определения ориентации анизотропных слоев.

На основе полученных оптимальных структур были изготовлены образцы углепластика с объемным содержанием МУНТ 0, 1 и 2 %. Проведена сканирующая электронная микроскопия с использованием FE-SEM Hitachi S-5500 для проверки однородности распределения и совместимости эпоксидной матрицы и МУНТ. Измерение α_x выполнено с помощью термомеханического анализатора TA Instruments Q400. Измеренные значения α_x находятся в диапазоне от $6,2 \cdot 10^{-8}$ до $1,98 \cdot 10^{-7}$ 1/К.

Подход к оптимизации структуры, предложенный в этой статье, позволяет получить набор решений со стабильно низким α_x в диапазоне до $1 \cdot 10^{-7}$ 1/К. Преобразование проектного пространства угловой ориентации слоев и ограничение области поиска позволило сократить диапазон рассматриваемых решений на 83,9 %.

© ПНИПУ

© Пасечник Кирилл Арнольдович – н.с., e-mail: pasechnik.kirill@gmail.com.

Обверткин Иван Владимирович – н.с., e-mail: +79632609742@yandex.ru.

Власов Антон Юрьевич – к.ф.-м.н., доц., e-mail: vlasov.anton@gmail.com.

Kirill A. Pasechnik – Researcher, e-mail: pasechnik.kirill@gmail.com.

Ivan V. Obvertkin – Researcher, e-mail: +79632609742@yandex.ru.

Anton Yu. Vlasov – CSc in Physical and Mathematical Sciences, Associate Professor, e-mail: vlasov.anton@gmail.com.



Эта статья доступна в соответствии с условиями лицензии Creative Commons Attribution-NonCommercial 4.0 International License (CC BY-NC 4.0)

This work is licensed under a Creative Commons Attribution-NonCommercial 4.0 International License (CC BY-NC 4.0)

NUMERICAL AND EXPERIMENTAL STUDY ON CFRP STRUCTURE OPTIMIZATION FOR COEFFICIENT OF THERMAL EXPANSION

K.A. Pasechnik, I.V. Obvertkin, A.Y. Vlasov

Reshetnev University, Krasnoyarsk, Russian Federation

ARTICLE INFO

Received: 15 January 2023
Approved: 25 May 2023
Accepted for publication:
15 June 2023

Keywords:

optimization of macrostructure of hybrid composite, stable low coefficient of thermal expansion of composite, MWCNTs, PCA, NSGA-II, Mori – Tanaka model.

ABSTRACT

This paper explores the optimization macrostructure to reach a stable low coefficient of thermal expansion α_x of a composite with carbon fibers. To limit the search area, a necessary condition for the existence of α_x local minima is proposed, expressed in terms of the radii of hyperspheres in the design space of the angular orientation of the layers transformed by the PCA algorithm. The analysis of the structure variants characterized by low α_x shows different sustainability to lamina properties variability. Multi-criteria optimization was carried out. The objective functions are expectation $E(\alpha_x)$ and variance $Var(\alpha_x)$. The analysis of Pareto fronts and probability density functions make it possible to estimate the reachability of the calculated α_x under given conditions of lamina properties variability.

The reduction variance opportunity of α_x distribution by modifying the polymer matrix with MWCNTs under conditions of reinforcing fibers disorientation and lamina properties variability is investigated. The microstructure modification of the polymer composite material allows to reduce the $Var(\alpha_x)$ by 91.61 % with a volume ratio of MWCNTs up to 1 %. Requirement thermomechanical properties are reached by determining the orientation of anisotropic layers.

Based on the obtained optimal structures, specimens of CFRP with 0, 1 and 2 vol.% MWCNTs were made. Scanning electron microscopy using FE–SEM Hitachi S–5500 was performed to check the uniformity of distribution and compatibility of the epoxy matrix and MWCNTs. The measurement of α_x is determined using a TA Instruments Q400 thermomechanical analyzer. Measured α_x of specimens is in the range from $6.2 \cdot 10^{-8}$ to $1.98 \cdot 10^{-7}$ 1/K.

The structure optimization approach proposed in this paper makes it possible to obtain a set of solutions with a consistently low α_x in the range up to $1 \cdot 10^{-7}$ 1/K. The transformation of the design space of the layers' orientation angles and the limitation of the search area allowed to reduce the range of solutions under consideration by 83.9 %.

© PNRPU

Introduction

The size changes control is very important in some applications, for example, in space structures. Zero thermal expansion materials is needed in structures subject to temperature changes such as a backplane support structure for a large space telescope, antenna booms, solar array frames and etc. Unlike classical materials, composite laminates can be designed in such a way as to reduce the coefficients of thermal expansion (CTE) in the desired direction to a specified value. This can be done by the appropriate sequence of laminate layers, the angular orientation of each layer and the microstructure properties control.

The structure optimization problem of a composite material to obtain the specified mechanical and thermomechanical properties has repeatedly attracted the attention of researchers [1–9]. To reduce the CTE value of CFRP, the researchers design a new kind of multi-functional curing agent for epoxy resin [10] or add inorganic particles such as carbon nanotubes, aluminum nitride, silicon dioxide, and so on [11–18]. There is increasing interest in combining reinforcement scales of nanoscale reinforcements with traditional micron-sized fibers [19; 20]. The authors of the work [21] evaluated the feasibility of using multi-walled carbon nanotubes (MWCNTs) for the control of coefficients of thermal expansion of composite materials. The use of MWCNTs aligned axially was shown

to be effective at controlling α_x of polymer composites. The authors theoretically calculated the MWCNT volume fraction at which α_x of composites based on different type of material and containing MWCNTs become zero. In particular, the authors determined the MWCNT content necessary for zero coefficients of thermal expansion to be about 10 vol.% in the polymer materials at temperature range of -5 °C to 85 °C. Inorganic compounds with negative thermal expansion (ZrW_2O_8 , ScF_3 , $Mn_{0.98}CoGe$, $Sm_{2.75}C_{60}$) can be used to compensate and control the CTEs of CFRP [22–29]. But for many inorganic NTE compounds, their CTE are small in magnitude or the effective temperature window is narrow [30; 31].

The orientation of fibers in composites may result in anisotropic thermal expansion has a small or even negative CTE value [33; 34]. Although the task of the composite's macrostructure optimization is complicated by the high sensitivity of the theoretically achieved near-zero coefficients of thermal expansion to the lamina properties variability, which inevitably present in practice due to disorientation of reinforcing fibers, and various degrees of cure, volume fraction, residual moisture and etc. However, to date, the literature has not considered the possibility of obtaining a hybrid composite with zero α_x , reinforced with carbon fibers in combination with MWCNTs, with an estimate of the density function of the probability distribution of α_x under the conditions of lamina properties variability and its disorien-

tation. This paper first describes the methodology of obtaining a layered composite with near zero α_x based on estimate $E(\alpha_x)$ and $Var(\alpha_x)$ as target parameters. Possibilities of reducing the variance of the target parameter by means of an integrated approach to determining the optimal orientation of layers of hybrid composites with different volume content of MWCNT is considered. A detailed description of the calculation procedure for the target parameters using randomly generated lamina's orientation angle error and lamina properties variability is presented in the next session. The results section discusses the possibility of reducing the $Var(\alpha_x)$ using MWCNTs, analyzing the Pareto-optimum front curves. Further, the experimental estimates of α_x of the composite are reported in detail.

1. Material and methods

This section details the specific materials, calculation and manufacturing processes used to create the carbon/epoxy laminated composites with a stable low coefficient of thermal expansion. This article analyzes composites with a symmetrical sequence of layers $[\pm \theta_1, \dots, \pm \theta_7]_s$. A total number of layers is 28 and a thickness of each layer is 0.152 mm. In this study, carbon fibers with following thermomechanical properties are used: $E_1=430$ GPa, $E_2=14$ GPa, $\nu_{12}=0.2$, $\nu_{23}=0.46$, $\nu_{13}=0.2$, $G_{12}=8.78$ GPa, $G_{23}=2.1$ GPa, $G_{13}=8.78$ GPa, $\alpha_1=-0.9 \cdot 10^{-6}$ K⁻¹, $\alpha_2=6.8 \cdot 10^{-6}$ K⁻¹ [13]. The matrix is mixture of epoxy resins based on bisphenol A and epichlorohydrin as well as aromatic and aliphatic diamines with following properties: $E_m=3.1$ GPa, $\nu_m=0.3$, $\alpha_m=65 \cdot 10^{-6}$ K⁻¹ [13]. As a nanoscale filler, we consider multi-walled carbon nanotubes of the "Taunit" series of the Nanotech Center LLC with an outer diameter of 20-50 nm and length of more than 2 μ m. Its Young's modulus and coefficient of thermal expansion at the room temperature are taken to be 1000 GPa and $-12 \cdot 10^{-6}$ K⁻¹ [21; 35; 36], respectively.

1.1. Calculation procedure

The search for the local minimum of α_x expectation and variance as objective functions is performed by two ways: 1. combination of PCA and gradient descent method and 2. NSGA-II. Searching algorithm was performed using "scikit-learn" to program PCA algorithm and multi-objective optimization framework "pymoo" [37] to program NSGA-II in Python. The mathematical expectation $E(\alpha_x)$ and the variance $Var(\alpha_x)$ are determined from the assumption of the variability of lamina properties and its disorientation. We assumed the standard deviation of properties equal to $s=2$, 4 and 10 percent of the value of the mathematical expectation. The sample of possible disorientation of layers was formed from the assumption of a normal distribution with parameters: $E=0$, $\sigma=2$.

The solutions to the optimization problem are the local minima of the nonlinear non-convex objective function in the design space of the layers' orientation angles for com-

posites with different microstructure modifiers. The objective function is nonlinear and non-convex, so the result of the gradient method strongly depends on the initial set of variables. Therefore, the gradient descent method must be repeated for different initial values of the angles. For the rational choice of initial values, the necessary condition for the existence of a local minimum in the vicinity of a certain point of the design space of angles meeting the requirement $\alpha_x < 1 \cdot 10^{-7}$ was formed using the PCA algorithm.

1.1.1. PCA and gradient descent method

The creation of the necessary condition for the existence of a local minimum was carried out in several stages for composites with different volume contents of MWCNTs ($V_{CNT}=0, 1$ and 2 %). The goal is to limit the search area of local minima. First, a representative sample of the stacking sequence of composite layers corresponding to a uniform distribution of the angles of each layer was formed for a composite with 0, 1 and 2 vol.% MWCNTs and the corresponding α_x were determined, according to CLT. The uniform distribution is constructed in the range from -90° to $+90^\circ$ and with the number of elements 10^6 . Using the PCA algorithm, two principal components were identified in the initial design space of the orientation of the layers. Next, the data is marked according to the condition $E(\alpha_x) < 1 \cdot 10^{-7}$ and the area of the variables value satisfying this condition is defined as a k -sphere with radius R in the new reduced PCA space. Consequently, the first stage of necessary condition for the existence of a local minimum can be written in term a new vector of principal components $x=(x_1, \dots, x_k)$. Principal components are linear combinations of initial features with coefficients, which can be represent as a set of size k of n -dimensional vectors of weights $w_{(k)}=(w_1, \dots, w_n)_{(k)}$ for $k=1, \dots, i$ corresponding to numbers of principal components of the reduced space and $n=1, \dots, t$ corresponding to numbers of initial features. The first stage of necessary condition:

$$\sum_{i=1}^k x_i^2 \leq R^2. \tag{1}$$

Condition (1) reduces the initial sample of the angle combination for stacking sequence. The subsequent reductions were performed by re-determining the principal components of the already reduced sample and determining the radius R_j , where j numbers of iteration. Accordingly, in general terms, the stages of implementing the necessary condition for the existence of a local minimum can be written as a sequence of conditions:

$$\sum_{i=1}^k x_i^{(1)2} \leq R_1^2 \wedge \sum_{i=1}^k x_i^{(2)2} \leq R_2^2 \wedge \dots \wedge \sum_{i=1}^k x_i^{(j)2} \leq R_j^2. \tag{2}$$

The angular orientation of the layers $\theta=(\theta_1, \dots, \theta_n)$ is expressed as a scalar product of matrices X and W , where x_j corresponding to coefficients of the principal components for a specific data point satisfying the requirements.

The formulated necessary conditions were used to form from the design space of the layers' orientation a sample of initial values of the angles to search for a local minimum of $E(\alpha_x)$. The sample of the initial angular orientation of the layers consisted of 10^6 elements. Further, for each element of the sample, a local minimum of the expectation function was found by the gradient method. The $Var(\alpha_x)$ was calculated for each local minimum.

$$E(\alpha_x) = f(\pm\theta_1, \dots, \pm\theta_n), \quad (3)$$

$$\theta_i = \theta_{i-1} - \lambda_i \nabla E(\alpha_x). \quad (4)$$

This method was repeated for composites with 1, 2 and 4 vol.% MWCNTs. The comparison of $E(\alpha_x)$ and $Var(\alpha_x)$ is performed in chapter 3. Stiffness tensor and α_x of carbon nanotube reinforced composites are modeled using the Mori – Tanaka theory based on Eshelby's inclusion theory.

1.1.2. NSGA-II

The construction of the optimum Pareto front showing the variance of CTE as a function of mathematical expectation was performed using the NSGA-II algorithm. For this problem we choose a population size of 10^2 and with only 30 offspring population size in each generation. The initial population consists of solutions with the lowest variance value obtained by the gradient method. A running performance metric [38] was used to assess the convergence and diversity of a generation set of non-dominated solutions. This metric can provide a generation-wise performance profile so that a more detailed understanding of the algorithm's performance. The running metric shows the difference in the objective space from one generation to another.

1.2. Materials characterization

1.2.1. Materials, composites manufacturing and specimen preparation

Composite material based on resin with 0, 1 and 2 vol.% MWCNTs was obtained. Before the introduction of MWCNTs into the epoxy resin, the functionalization was performed to add functional oxygen-containing groups to the surface of the modifier. The chemistry modification included holding at 35°C for 7 days in methylene chloride under reflux. Then carbon nanoparticles were sonicated in a water bath in concentrated sulfuric and nitric acid in a ratio of 3 to 1 for 3 hours after filtration in vacuum and washing with distilled water. Then carbon nanoparticles were collected and dried on calcium chloride and silica gel.

The MWCNTs were weighed and mixed with the epoxy resin to achieve final target weight fractions of 0.114 and 0.227 %. The homogenizer IKA T18 was used to mixing. After dispersion, the mixture was degassed under vacuum for 10 min and the curing agent was added to the dispersion and mixed using high-speed propeller agitator. Layers of

UD carbon fibers were manually laid on the mold in compliance with the calculated stacking sequence and impregnated with dispersion. After curing the polymer at 120°C for 12 hours, 5 samples with dimensions of 5x15 mm were cut from composites with 0, 1 and 2 vol.% MWCNTs.

1.2.2. Scanning electron microscopy

The morphology of prepared material was characterized by the Scanning electron microscopy using FE–SEM Hitachi S–5500 instrument (Japan) operating at 5 kV. The composite specimens were delaminated after freezing in liquid nitrogen for 2 min. Before examination, the composite samples were glued to a support and to minimize sample charging coated with platinum by magnetron sputtering during 1 min at the current of 10 mA and in a vacuum of $8 \cdot 10^{-6}$ Bar in argon atmosphere. To view the hierarchical morphology of the composites, fracture surfaces were imaged.

1.2.3. Thermomechanical analysis

The coefficient of thermal expansion of the manufactured samples was determined using a TA Instruments Q400 thermomechanical analyzer. The tests were carried out in two stage. The first stage consists in heating at a heating rate of 5°C/min up to 100°C and subsequent isothermal exposure for 350 min in a nitrogen environment to stabilize the size of the samples as a result of removing the remaining moisture. The second stage consists of cooling to 40°C, isothermal exposure for 20 min and subsequent heating to 100°C to measure α_x . The second stage was several times repeated to obtain a stable measurement result.

2. Results

2.1. Calculation results

2.1.1. The result of applying the necessary condition for near-zero CTE

Fig. 1 shows the result of identification the two main components of the layer orientation space for a composite with native resin (with 0 vol.% MWCNT) using the PCA algorithm. Labeling the data of the initial sample in accordance with condition $E(\alpha_x) < 1 \cdot 10^{-7}$ makes it possible to identify a pattern in the angular orientation of the layers, expressed in the components of the reduced space.

The sequential reduction of the initial sample by the definition of the principal components of the variable space and the determination of acceptance region as a circle with radius R leads to the formation of the necessary condition for the existence of a local minimum satisfying the condition $E(\alpha_x) < 1 \cdot 10^{-7}$. The range of acceptable values of variables can be indicated by a circle with a radius of 2.48–3.02 and radius of hypersphere 2.17–2.66 in case of 2 and 7 principal components, respectively.

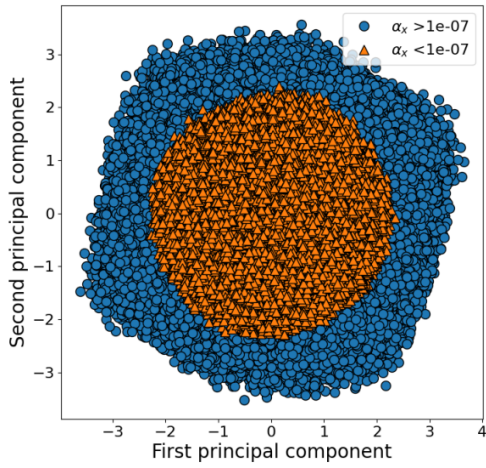


Fig. 1. CTE of multilayer composite as a function of layer orientation in the design space with two principal components

The distribution density R of the hypersphere surface satisfying the condition $E(\alpha_x) < 1 \cdot 10^{-7}$ is shown in the Fig. 2. Fig. 3 shows the coordinates of the vectors w_i . For the composite considered in this paper, the necessary condition for the existence of a near-zero α_x can be formed as a weighted sum of vectors of principal components whose number is equal to the number of initial variables:

$$R_1^2 \leq \sum_{i=1}^k x_i^2 \leq R_2^2, \quad (5)$$

$$\theta = x_i w_k.$$

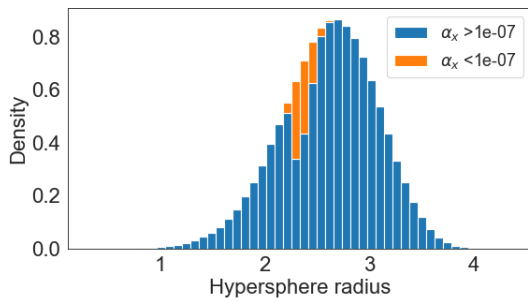


Fig. 2. Distribution density R of the hypersphere surface

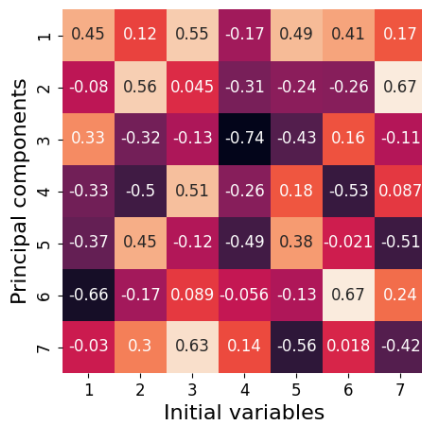


Fig. 3. Heatmap of principal components for a data set

Using the gradient method, the layer orientations for local minima and the corresponding variance are determined. Comparison of the found points of the design space indicates different variability of the objective function (Fig. 4). The vast majority of $E(\alpha_x)$ are in the range $1 \cdot 10^{-9} - 1 \cdot 10^{-7}$ and are uniformly distributed in the space of variables. Under the conditions of a given a priori variability of properties (σ), $Var(\alpha_x)$ is equal to $1 \cdot 10^{-16} - 1 \cdot 10^{-14}$. The obtained samples of the sequence of layers for the native composite and composites with 1, 2 and 4 vols.% are used as the initial population for the genetic algorithm of multicriteria optimization to find the Pareto front of expectation and variance.

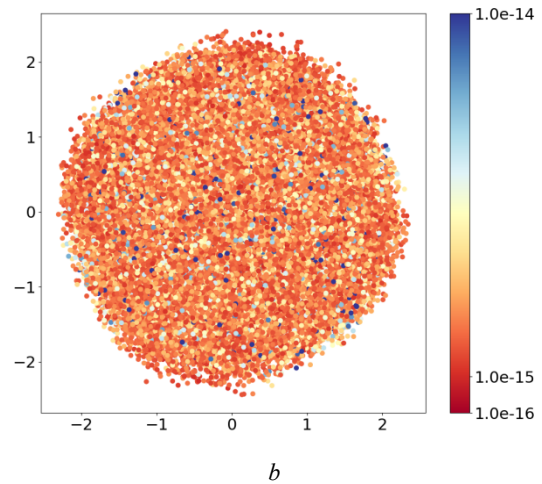
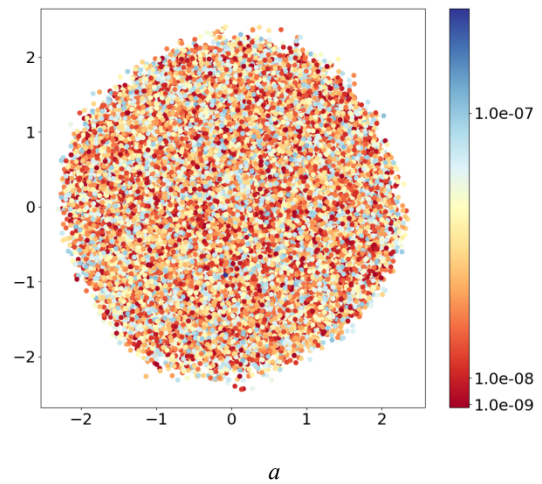


Fig. 4. $E(\alpha_x)$ (a) and corresponding $Var(\alpha_x)$ (b) under conditions of variability of lamina properties and its disorientation for the native composite

2.1.2. NSGA-II

Fig. 6 shows a comparison of the Pareto fronts obtained using the NSGA-II algorithm for various cases of a priori variability of the properties of the composite lamina. The final solutions ($V_{CNT}=0, s=2\%$) in the objective space for native composites is slightly convex Pareto fronts, which in the area from $7.78 \cdot 10^{-7}$ to $8.09 \cdot 10^{-10}$ demonstrate an almost linear relationship between the CTE expectation and its variance.

In the range from $8.09 \cdot 10^{-10}$ to $1.73 \cdot 10^{-12}$, the variance increases sharply, asymptotically approaching the ordinate axis. Pareto optimal solutions for composites with 1 vol.% MWCNTs form front characterized by a decrease in the average variance of the sample by 91.61 %. The Pareto front found for a composite with 2 vol.% MWCNTs is discontinuous, the average variance of which decreased by 70.48 % compared to the native composite.

With the growth of a priori variability of the lamina properties to $s=4\%$ and $s=10\%$, the Pareto front acquires a pronounced convex shape and a significant increase in the variance of the objective function is observed. With an increase in the a priori dispersion of properties from 2 to 4 %, the average variance of the Pareto front increases by 72 %. The Pareto front found for a composite with 2 vol.% MWCNTs is concave in the range from $4 \cdot 10^{-7}$ to $1 \cdot 10^{-7}$. With a decrease in $E(\alpha_x)$, the variance increases sharply, asymptotically approaching the ordinate axis. With an increase in the a priori dispersion of properties from 4 to

10 %, the average variance of the Pareto front increases by 85 %. Visualizations of the running performance metric demonstrate convergence during an early phase of the algorithm (Fig. 5).

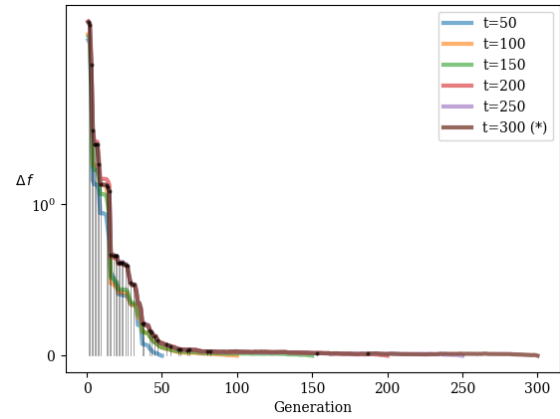


Fig. 5. The running performance metric

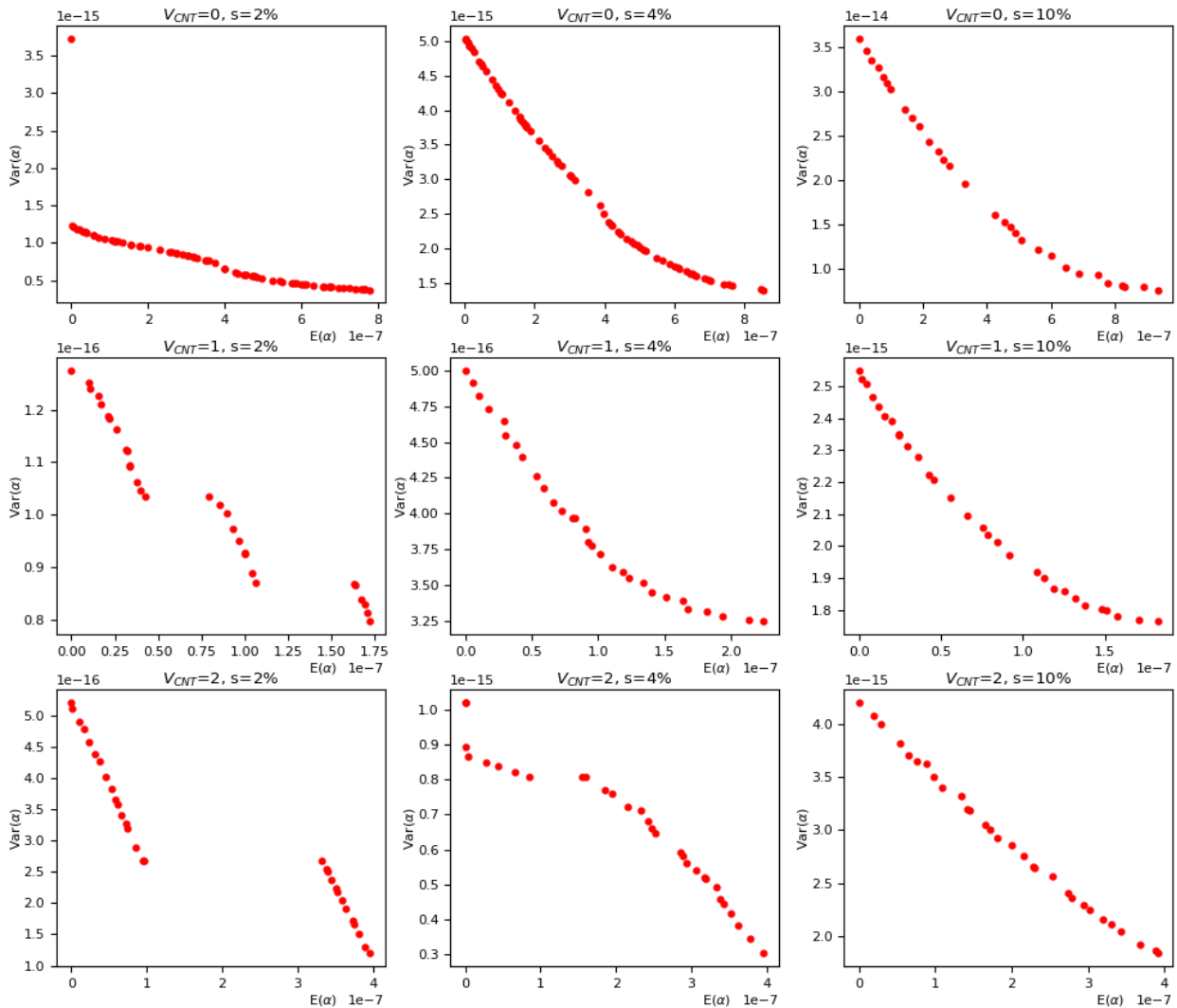


Fig. 6. Pareto fronts of two objective functions: expectation of coefficient of thermal expansion and variance

Probability density functions for α_x of the composite is close to the normal distribution. For the experimental evaluation of the calculated sequence of layers, several specimen of material were made. Scheme 1: native composite with the following stacking sequence $[\pm 15.7, \pm 86.2, \pm 12.4, \pm 58.7, \pm 13.4, \pm 23.0, \pm 48.9]_s$. Scheme 2: composite with 1 vol.% MWCNTs with stacking sequence $[\pm 10.8, \pm 42.1, \pm 25.6, \pm 24.1, \pm 40.7, \pm 16.1, \pm 84.8]_s$. Scheme 3: composite with 2 vol.% MWCNTs with stacking sequence $[\pm 72.6, \pm 1.8, \pm 2.7, \pm 1.5, \pm 7.8, \pm 0.7, \pm 13.2]_s$. Calculated values of objective functions for Scheme 1: $E(\alpha_x)=-1.78 \cdot 10^{-7}$, $Var(\alpha_x)=1.7 \cdot 10^{-15}$. Scheme 2: $E(\alpha_x)=2.3 \cdot 10^{-8}$, $Var(\alpha_x)=6.37 \cdot 10^{-16}$. Scheme 3: $E(\alpha_x)=7.4 \cdot 10^{-7}$, $Var(\alpha_x)=6.05 \cdot 10^{-16}$. Measured α_x is presented in chapter 2.3.

2.2. Composite microstructure characterization

Fig. 7, *a*, shows the cryo-fracture surface of the multiscale composites with carbon fibers and 2 vol.% MWCNTs dispersed in epoxy matrix. MWCNTs are randomly distributed in the polymer matrix to form zones with different volume contents of nanoparticles (Fig. 7, *b*, and 7, *c*). The approximate concentration of MWCNTs in the ag-

glomerates is up to 8 % (Fig. 7, *d*). The fracture surface demonstrates brittle fracture in areas with a low volume content of nanoparticles (Fig. 7, *c*) and a large surface roughness for MWCNTs agglomeration zones (Fig. 7, *d*). The higher magnification image in Fig. 7, *b*, shows MWCNTs on the fracture surface that are relatively short and shows minimal nanotube pullout, suggesting a relatively strong interaction between MWCNTs and the epoxy matrix.

2.3. Thermomechanical analysis

Measured α_x of specimen is in the range from $6.2 \cdot 10^{-8}$ to $1.98 \cdot 10^{-7}$. The size change demonstrates a non-linear nature, which is explained by the complexity of measuring small α_x , due to factors such as the unevenness of the temperature field around the measured specimen and the loss of residual moisture, which are invisible when measuring large moduli α_x . In order to reduce the influence of the factors, a long exposure time was used before and after the temperature change to stabilize the specimen size. Fig. 8 shows a complete measurement cycle consisting of two stages. The first stage is desorption of residual moisture. The second stage is sequential heating and cooling to measure the α_x .

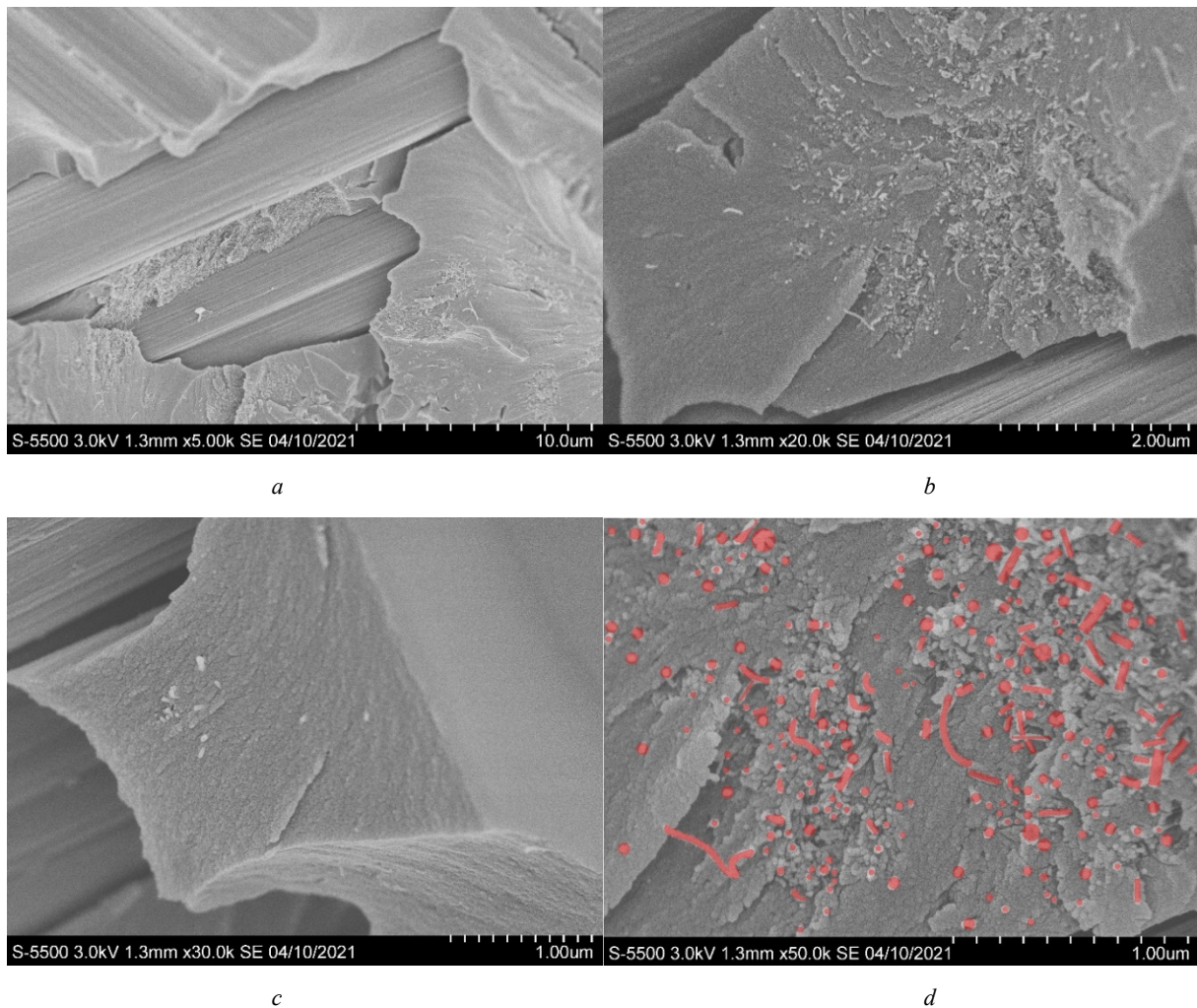


Fig. 7. Cryo-fracture surface of the multiscale composites with carbon fibers and 2 vol.% MWCNTs

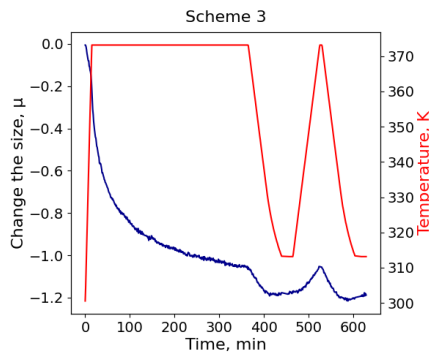


Fig. 8. The cycle of measuring α_x of CFRP

Fig. 9 shows the measured change in the size of the composite after stabilization of its dimensions due to moisture loss. Scheme 1: $\alpha_x \approx 6.2 \cdot 10^{-8}$. Scheme 2: $\alpha_x \approx 1.39 \cdot 10^{-7}$. Scheme 3: $\alpha_x \approx 1.98 \cdot 10^{-7}$.

Discussion and conclusions

As shown in the Fig. 6, optimization problems of minimizing the α_x function is actually a multi-criteria optimization, the objective functions of which are the mathematical expectation $E(\alpha_x)$ and variance of mathematical expectation $Var(\alpha_x)$. This approach makes it possible to analyze the Pareto front and probability density functions for the α_x in order to assess the reachability of the calculated values under given conditions of property variance.

The objective function is nonlinear and non-convex (Fig. 4), so the result of the gradient method strongly depends on the initial set of variables and must be repeated for different initial values of the angles. The reduction of the

search area for local minima can be reduced by analyzing the design space with the PCA algorithm and forming the necessary conditions for the existence of a local minimum. It is proposed to limit the search area in the project space by introducing two parameters R_1 and R_2 , which are the radii of the external and internal hypersphere limiting the area of the design space of the layers' orientation angles (Fig. 2).

As we can see from the chart presented above (Fig. 6), the microstructure modification of the polymer composite material allows to reduce the $Var(\alpha_x)$ by 91.61 % with a volume ratio of MWCNTs up to 1 %. In addition to the requirements for thermal behavior, it is important to consider more general elastic properties. Resin modification with the addition of MWCNTs slightly increases the CTE and the effective stiffness of the lamina in the longitudinal direction, and significantly reduces the CTE in the transversal direction, which together causes a change in the optimal reinforcement architecture – the angle reduction between the reinforcing fibers direction and the direction of the longitudinal axis of the material. Consequently, the material has a large longitudinal elastic modulus, while, due to the reduction of the CTE of the lamina in the transversal direction, it has a lower variance of the CTE compared to the non-modified composite.

The calculated CTEs of unidirectional laminas with modified and non-modified resin show high convergence with the experimental data. As a next step, it is necessary to check the obtained calculated stacking sequence of layers on a significant series of samples, sufficient to confirm the stability of the researched parameter. It is important to continue research on effective reinforcement architectures using alternative analytical methods of machine learning to find more complicated stacking sequence.

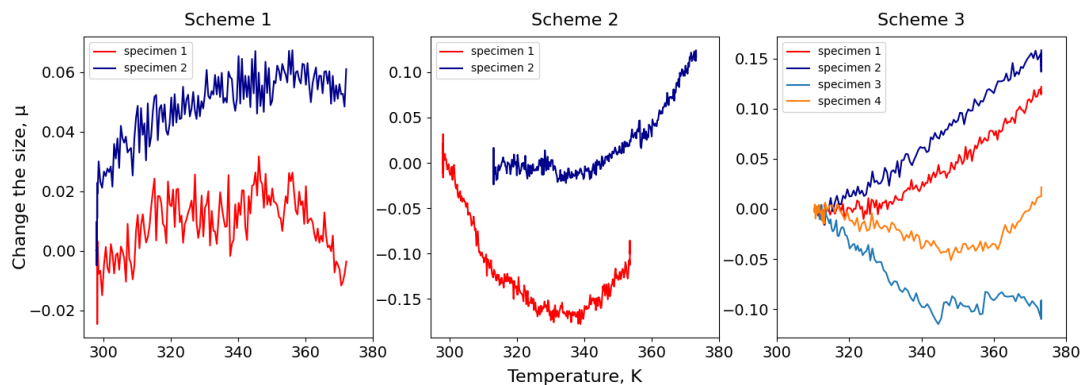


Fig. 9. Measured α_x of CFRP

References

1. Anaya L., Vicente W., Pavanello R. Minimization of the Effective Thermal Expansion Coefficient of Composite Material Using a Multi-scale Topology Optimization Method. *EngOpt 2018 Proceedings of the 6th International Conference on Engineering Optimization* / ed. Rodrigues H.C. et al. Cham: Springer International Publishing, 2019, pp. 1055–1060. https://doi.org/10.1007/978-3-319-97773-7_91

2. Zhengchun D. et al. Design and application of composite platform with extreme low thermal deformation for satellite. *Compos. Struct. Elsevier Ltd*, 2016, Vol. 152, pp. 693–703. <https://doi.org/10.1016/j.compstruct.2016.05.073>

3. Catapano A., Desmorat B., Vannucci P. Stiffness and Strength Optimization of the Anisotropy Distribution for

Laminated Structures. *J. Optim. Theory Appl.* 2015, Vol. 167, № 1, pp. 118–146. <https://doi.org/10.1007/s10957-014-0693-5>

4. Kim D. et al. Topology optimization of functionally graded anisotropic composite structures using homogenization design method. *Comput. Methods Appl. Mech. Eng. Elsevier B.V.*, 2020, Vol. 369, pp. 113220. <https://doi.org/10.1016/j.cma.2020.113220>

5. Schaedler de Almeida F. Optimization of laminated composite structures using harmony search algorithm. *Compos. Struct. Elsevier Ltd.*, 2019, Vol. 221, pp. 110852. <https://doi.org/10.1016/j.compstruct.2019.04.024>

6. Peng X. et al. Multiple-scale uncertainty optimization design of hybrid composite structures based on neural network and genetic algorithm. *Compos. Struct. Elsevier Ltd.*, 2020, Vol. 262, pp. 113371. <https://doi.org/10.1016/j.compstruct.2020.113371>

7. Hao P. et al. Efficient reliability-based design optimization of composite structures via isogeometric analysis // *Reliab. Eng. Syst. Saf. Elsevier Ltd.*, 2021, Vol. 209, pp. 107465. <https://doi.org/10.1016/j.ress.2021.107465>

8. das Neves Carneiro G., Conceição António C. Dimensional reduction applied to the reliability-based robust design optimization of composite structures. *Compos. Struct. Elsevier Ltd.*, 2021, Vol. 255, pp. 112937. <https://doi.org/10.1016/j.compstruct.2020.112937>

9. Sigmund O., Torquato S. Design of materials with extreme thermal expansion using a three-phase topology optimization method. *J. Mech. Phys. Solids. Elsevier Ltd.*, 1997, Vol. 45, № 6, pp. 1037–1067. [https://doi.org/10.1016/S0022-5096\(96\)00114-7](https://doi.org/10.1016/S0022-5096(96)00114-7)

10. Q.S. Sun, Y.D. Feng, J. Guo, et al. High performance epoxy resin with ultralow coefficient of thermal expansion cured by conformation-switchable multi-functional agent. *Chemical Engineering Journal*, 2022, Vol. 450, pp. 138295. <https://doi.org/10.1016/j.cej.2022.138295>

11. S.R. Wang, Z.Y. Liang, P. Gonnet, Y.H. Liao, B. Wang, C. Zhang. Effect of nanotube functionalization on the coefficient of thermal expansion of nanocomposites. *Adv. Funct. Mater.*, 2007, 17(1), pp. 87-92. <https://doi.org/10.1002/adfm.200600760>

12. J.K. Ma, T.Y. Shang, L.L. Ren, Y.M. Yao, T. Zhang, J.Q. Xie, B.T. Zhang, X.L. Zeng, R. Sun, J.B. Xu, C.P. Wong. *Through-plane assembly of carbon fibers into 3D skeleton achieving enhanced thermal conductivity of a thermal interface material.* *Chem. Eng. J.*, 2020, 380, p. 8. <https://doi.org/10.1016/j.cej.2019.122550>

13. Obvertkin, I., K. Pasechnik, и A. Vlasov. The potential of using SWCNTs, MWCNTs and CNFs capable of increasing the composite material dimensional and technological stability as modifiers of a polymer matrix. *PNRPU Mechanics Bulletin*, 2021, № 4, pp. 98-110. <https://doi.org/10.15593/perm.mech/2021.4.10>

14. K.C. Yung, B.L. Zhu, T.M. Yue, C.S. Xie. Effect of the Filler Size and Content on the Thermomechanical Properties of Particulate Aluminum Nitride Filled Epoxy Composites. *J. Appl. Polym. Sci.*, 2010, 116 (1), pp. 225-236. <https://doi.org/10.1002/app.31431>

15. C.J. Huang, S.Y. Fu, Y.H. Zhang, B. Lauke, L.F. Li, L. Ye. Cryogenic properties of SiO₂/epoxy nanocomposites. *Cryogenics*, 2005, 45 (6), pp. 450-454. <https://doi.org/10.1016/j.cryogenics.2005.03.003>

16. Ghasemi A.R., Mohammadi M.M., Mohandes M. The role of carbon nanofibers on thermo-mechanical properties of polymer matrix composites and their effect on reduction of residual stresses. *Compos Part B Eng.*, 2015, no. 77, pp. 519-27. <https://doi.org/10.1016/j.compositesb.2015.03.065>

17. Shokrieh M.M., Akbari S., Daneshvar A. Reduction of residual stresses in polymer composites using nano-additives. *Residual Stress Compos Mater.*, 2014, pp. 350-73. <https://doi.org/10.1016/B978-0-12-818817-0.00013-5>

18. Pan J., Bian L. A physics investigation for influence of carbon nanotube agglomeration on thermal properties of composites. *Mater ChemPhys*, 2019, №. 236, <https://doi.org/10.1016/j.matchemphys.2019.121777>

19. Green K.J. et al. Multiscale fiber reinforced composites based on a carbon nanofiber/epoxy nanophased polymer matrix: Synthesis, mechanical, and thermomechanical behavior. *Compos. Part A Appl. Sci. Manuf. Elsevier*, 2009, Vol. 40, № 9, pp. 1470–1475. <https://doi.org/10.1016/j.compositesa.2009.05.010>

20. Fu S. et al. Some basic aspects of polymer nanocomposites: A critical review. *Nano Mater. Sci. Elsevier BV*, 2019. Vol. 1, № 1, pp. 2–30. <https://doi.org/10.1016/j.nanoms.2019.02.006>

21. Shirasu K. et al. Negative axial thermal expansion coefficient of carbon nanotubes: Experimental determination based on measurements of coefficient of thermal expansion for aligned carbon nanotube reinforced epoxy composites. *Carbon N. Y. Elsevier Ltd.*, 2015, Vol. 95, pp. 904–909. <https://doi.org/10.1016/j.carbon.2015.09.026>

22. J.C. Lin, P. Tong, K. Zhang, H.Y. Tong, X.G. Guo, C. Yang, Y. Wu, M. Wang, S. Lin, L. Chen, W.H. Song, Y.P. Sun. Colossal negative thermal expansion with an extended temperature interval covering room temperature in fine-powdered Mn_{0.98}CoGe. *Appl. Phys. Lett.*, 2016, 109 (24), p. 5. <https://doi.org/10.1063/1.4972234>

23. V.K. Thakur, Y.Z. Li, H.C. Wu, M.R. Kessler. Synthesis, characterization, and functionalization of zirconium tungstate (ZrW₂O₈) nano-rods for advanced polymer nanocomposites. *Polym. Adv. Technol.*, 2017, 28 (11), pp. 1375-1381. <https://doi.org/10.1002/pat.4014>

24. T.A. Mary, J.S.O. Evans, T. Vogt, A.W. Sleight. Negative Thermal Expansion from 0.3 to 1050 Kelvin in ZrW₂O₈, *Science*, 1996, 272, p. 90. <https://doi.org/10.1126/science.272.5258.90>

25. B.K. Greve, K.L. Martin, P.L. Lee, P.J. Chupas, K.W. Chapman, A.P. Wilkinson. Pronounced Negative Thermal Expansion from a Simple Structure: Cubic ScF₃. *J. Am. Chem. Soc.*, 2010, 132, p. 15496. <https://doi.org/10.1021/ja106711v>

26. Zheng, X., Kubozono, H., Yamada, H. et al. Giant negative thermal expansion in magnetic nanocrystals. *Nature Nanotech* 3, 724–726 (2008). <https://doi.org/10.1038/nnano.2008.309>

27. X. Chu, Z. Wu, C. Huang, R. Huang, Y. Zhou, L. Li. ZrW₂O₈-doped epoxy as low thermal expansion insulating materials for superconducting feeder system. *Cryogenics*, 2012, 52(12), pp. 638-641. <https://doi.org/10.1016/j.cryogenics.2012.04.016>

28. P. Badrinarayanan, M. Rogalski, H. Wu, X. Wang, W. Yu, M.R. Kessler. Epoxy Composites Reinforced with Negative-CTE ZrW₂O₈ Nanoparticles for Electrical Applications. *Macromol. Mater. Eng.*, 2013, 298 (2), pp. 136-144.

29. Y.Y. Zhao, F.X. Hu, L.F. Bao, J. Wang, H. Wu, Q.Z. Huang, R.R. Wu, Y. Liu, F.R. Shen, H. Kuang, M. Zhang, W.L. Zuo, X. Q. Zheng, J.R. Sun, B.G. Shen. Giant Negative Thermal Expansion in Bonded MnCoGe-Based Compounds with Ni₂In-Type Hexagonal Structure. *J. Am. Chem. Soc.*, 2015, 137 (5), pp. 1746-1749. <https://doi.org/10.1002/mame.201100417>

30. L.A. Neely, V. Kochergin, E.M. See, H.D. Robinson. Negative thermal expansion in a zirconium tungstate/epoxy composite at low temperatures. *J. Mater. Sci.*, 2014, 49 (1), pp. 392-396. <https://doi.org/10.1007/s10853-013-7716-8>

31. J. Arvanitidis, K. Papagelis, S. Margadonna, K. Prassides, A.N. Fitch. Temperature-induced valence transition and associated lattice collapse in samarium fulleride. *Nature*, 2003, 425, p. 599. <https://doi.org/10.1038/nature01994>

32. K. Shirasu, A. Nakamura, G. Yamamoto, T. Ogasawara, Y. Shimamura, Y. Inoue, T. Hashida. Potential use of CNTs for production of zero thermal expansion coefficient composite

materials: An experimental evaluation of axial thermal expansion coefficient of CNTs using a combination of thermal expansion and uniaxial tensile tests. *Compos. Pt. A-Appl. Sci. Manuf.*, 95 (2017), pp. 152-160. <https://doi.org/10.1016/j.compositesa.2016.12.027>

33. R.P. Zhu, C.T. Sun. Effects of Fiber Orientation and Elastic Constants on Coefficients of Thermal Expansion in Laminates. *Mech. Adv. Mater. Struct.*, 10 (2) (2003), pp. 99-107. <https://doi.org/10.1080/15376490306733>

34. Yoon KJ, Kim J-S. Prediction of Thermal Expansion Properties of Carbon/Epoxy Laminates for Temperature Variation. *Journal of Composite Materials*. 2000;34(2):90-100. <https://doi.org/10.1177/002199830003400201>.

35. Polymer nanocomposites. *MRS Bull*, 2007, № 32, pp. 314-319. <https://doi.org/10.1557/mrs2007.229>.

36. Chang T., Gao H. Size-dependent elastic properties of a single-walled carbon nanotube via a molecular mechanics model. *J MechPhys Solids*, 2003, №. 51, pp. 1059-74. <https://doi.org/10.1016/S0022-5096>.

37. J. Blank and K. Deb, pymoo: Multi-Objective Optimization in Python. *IEEE Access*, Vol. 8, pp. 89497-89509, 2020. *Polym. Adv. Technol.*, 2017, 28 (11), pp. 1375-1381. <https://doi.org/10.1109/ACCESS.2020.2990567>

38. Blank, Julian and Kalyanmoy Deb. A. Running Performance Metric and Termination Criterion for Evaluating Evolutionary Multi- and Many-objective Optimization Algorithms. *2020 IEEE Congress on Evolutionary Computation (CEC)*, 2020, pp. 1-8. <https://doi.org/10.1109/CEC48606.2020.9185546>.

Финансирование. Работа выполнена за счет средств Программы стратегического академического лидерства СибГУ им. М.Ф. Решетнева («ПРИОРИТЕТ-2030»).

Конфликт интересов. Авторы заявляют об отсутствии конфликта интересов.

Вклад авторов равноценен.

Financing. The work was carried out at the expense of the Strategic Academic Leadership Program of Reshetnev University ("PRIORITY-2030").

Conflict of interest. The authors declare no conflict of interest.

The contribution of the authors is equivalent.